

AUTOMATIC 3D EXTRACTION OF RECTANGULAR ROADMARKS WITH CENTIMETER ACCURACY FROM STEREO-PAIRS OF A GROUND-BASED MOBILE MAPPING SYSTEM

^{1,2}B. Soheilian , ¹N. Paparoditis , ¹D. Boldo , ²J.P. Rudant

¹Institut Géographique National / MATIS, 2-4 Ave Pasteur, 94165 Saint-Mandé France

²Université de Marne-La-Vallée, Laboratoire Géomatériaux et Géologie de l'Ingénieur, 5 Bd Descartes, 77454 Marne la Vallée France
(bahman.soheilian , nicolas.paparoditis , didier.boldo)@ign.fr , jean-paul.rudant@univ-mlv.fr

KEY WORDS: close range photogrammetry, computer vision, mobile mapping system, stereo-matching, 3D object reconstruction, 3D perceptual grouping, roadmark, zebra-crossing, dashed-line.

ABSTRACT:

The present paper is an extension of a previous work presented in (Soheilian et al., 2006a) in which an automatic algorithm of zebra-crossing reconstruction from stereo-pairs of a mobile mapping system was proposed. The method has been adapted to reconstruct different types of rectangular roadmarks. The algorithm can be summarized in three main points. First of all a 3D edge point reconstruction is performed by a dynamic programming optimization matching conjugate epipolar lines. Then during a detection step, a dashed-line signature is recognized and sets of candidate line-segments are provided. A final modelling step rebuilds optimally each strip of the detected dashed-line. The method is evaluated on a set of 150 stereo-pairs. It provides promising results with a detection rate which is higher than 86%. Geometric accuracy of the method is about 2 *cm* for all of the reconstructed zebra-crossing and dashed-lines strips.

1 INTRODUCTION

Mobile mapping systems (El-Sheimy, 1996) are more and more used in road database generation and update. A mobile mapping system (MMS) generally consists of a vehicle equipped with data acquisition systems like Laser scanners and cameras. It is also equipped with georeferencing devices like GPS (Global Positioning System) and INS (Inertial Navigation System). Different kinds of MMS from data acquisition and positioning systems points of views are used in road modelling.

In a real time system presented in (Goulette et al., 2006), a laser scanner and direct localization sensors (GPS/INS) are used to acquire a 3D point cloud of the city. Within scanned point cloud, the road points are segmented automatically and some useful information such as road borders, width and curvature are computed.

In the system proposed by (Roncella and Forlani, 2006) a stereoscopic image-based system is applied for countryside roads surveying. A semi-automatic image processing method is then used to measure lane width with 10 *cm* accuracy.

Another MMS that is generally used for road monitoring is presented in (Barsi et al., 2006). The acquisition system is a combination of a pair of stereo-images and a set of laser projectors. The so called system provides the post-processing for the cross and longitudinal section extraction and crack detection.

In all of these mentioned applications, georeferencing is based only on direct positioning tools such as GPS and INS. However in dense urban areas the GPS signals are interrupted by high buildings which leads into the corruption of positioning process. In this case the absolute accuracy of positioning could reach 1 m or more for long interruptions.

The aim of the project in which this work takes place is to generate automatically 3D road databases in urban areas with a centimetre accuracy. Nevertheless on the one hand, direct positioning does not provide sufficient accuracy, on the other hand road borders are always occluded by cars and could not be extracted.

The roadmarks are useful features that are available on the majority of urban roads. Their size and shape are governed by strict specifications. The present work focuses on roadmark reconstruction for three following reasons:

1. In our system, roadmarks are used to improve the positioning of system into a centimeter accuracy. It is performed by matching roadmarks reconstructed from terrestrial images of MMS with the same roadmarks reconstructed from calibrated aerial images (Tournaire et al., 2006).
2. After road borders the roadmarks are the only features that can specify a road with centimetric accuracy. Moreover they give useful information about the number of lanes and their width.
3. There is a growing need for roadmark databases in autonomous navigation projects and driver assistance systems.

This paper is an extension of our previous algorithm of zebra-crossing reconstruction (Soheilian et al., 2006a) to rebuild different types of dashed-lines. similar to the algorithm developed for zebra-crossings reconstruction the output is a set of 3D models for each strip. More evaluations are then presented on a set of 150 images.

2 THE STRATEGY

2.1 Available data

Our MMS called *Stereopolis* (Paparoditis et al., 2005) is developed at the MATIS laboratory of IGN (See Figure1(a)). It consists of three stereoscopic rigs of 4000 × 4000 CCD cameras. The vertical rigs take images of the facades. The horizontal stereo-base provides stereo-images of road. The six cameras are perfectly synchronized (10 μ s) and provide very high quality images (SNR = 300 and 12 bits dynamic range). The system is also

equipped with 2 GPS antennas. The inputs of our roadmark reconstruction algorithm are the stereo-pairs provided by horizontal base of *Stereopolis* at their full resolution. (See Figure 1(b)). The interior calibration and relative orientation of the rig are *a priori* estimated and supposed to be rigid.



(a)



(b)

Figure 1: (a) *Stereopolis* MMS, (b) a stereo-pair captured by horizontal base.

2.2 Algorithm overview

The algorithm as depicted in the diagram of the figure 2 consists of three main steps of 3D edge chain reconstruction, different roadmark detection and strip modelling. Comparing to our previous work (Soheilian et al., 2006a) the first stays unchanged. The detection step is generalized to recognize dashed-lines and to provide a set of line-segments as hypothetical candidates for each strip. So in the modelling step compared to the previous work carried out for the zebra-crossing modelling, only the strip size parameters is changed. The output is a set of 3D strips.

3 3D EDGE CHAINS RECONSTRUCTION

As explained in our previous work (Soheilian et al., 2006a) the reconstruction step which is based on edge point matching between stereo-images can be summarized in :

- Edge detection in each image,
- Limitation of matching search area to an area around the road,
- Using correlation score to compute the initial matching cost,
- Final matching cost computed by taking into account the form continuity,

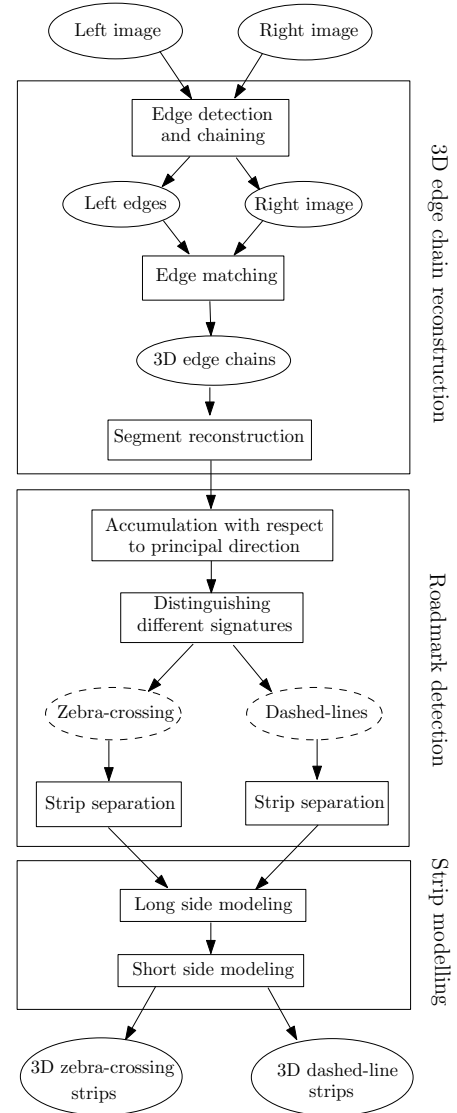


Figure 2: Our zebra-crossing and dashed-line strip reconstruction strategy.

- Matching by total cost minimization using dynamic programming.

The output of matching step is a set of 3D edge chains. A set of line-segments is then estimated by polygonization. The Figure 3 shows the reconstructed edge chains corresponding to stereo-pair seen in Figure 1(b).

4 DASHED-LINE DETECTION

As zebra-crossing and dashed-line strips are parallelogram patterns, we try to detect the 4 corners of each strip. However the strip corners are often damaged and do not respect the theoretical pattern. Moreover even if an undamaged strip is partially occluded by cars or pedestrians, the corner detection will fail. This is the reason why corner detection algorithms are not suitable for strip detection. Our solution is to find each pair of parallel sides and to reconstruct the corners by intersecting edge sides. Regarding the results of reconstruction step the main difficulties of strip side detection are:

- The reconstructed set contains too many irrelevant objects such as cars, pedestrians, local textures, etc.

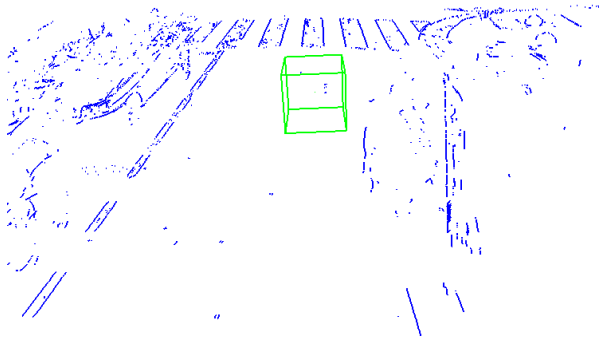


Figure 3: Reconstructed 3D edges.

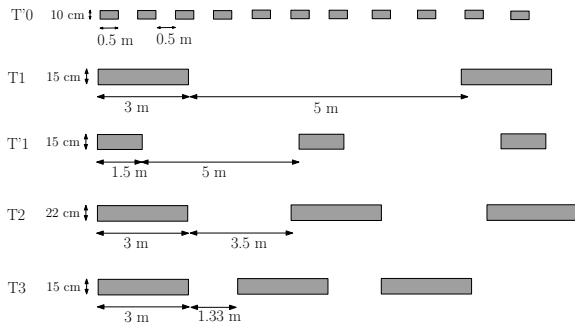


Figure 4: Specification of different types of dashed-lines.

- The chains are often fragmented due to edge detection and matching steps.
- The transversal sides of strips are not often correctly reconstructed due to the fact that they are aligned with epipolar lines.

In the detection step the two long sides that are rarely parallel to epipolar lines are detected and the transversal sides are detected by searching around the extremities of detected long sides. So only the two first difficulties must be handled.

Dashed-line strip detection algorithm is very similar to the detection of zebra-crossing strips. However because of their shorter length and their relative aligned position that is different from zebra-crossing strips some adaptations have to be made. In section 4.1 the known specifications of dashed-lines are presented. Section 4.2 begins with a short summary of our previous detection method. Then the performed adaptations for dashed-line detections are explained.

4.1 Dashed-lines specifications

In France roadmarks are painted on the roads according to strict specifications (Transport Ministry and Interior Ministry, 1988). For each type of dashed-line, their strips' length, width and also their inter-distance are known (see figure 4).

4.2 Dashed-line strip detection

In order to cut-down the complexity, all the reconstructed line-segments are projected on an approximate plane road and the detection step is performed in this 2D space. The approximate plane road is close enough to road surface so the deformation due to projection is negligible. The initial 3D coordinates are saved in an appropriate data structure in order to refine the final modelling. Like zebra-crossing strips, dashed-line strips are

always aligned with road direction. Indeed road direction is the most occurring direction within the line-segments and can be estimated automatically. We define a one-dimensional accumulation space in the perpendicular direction to road. This accumulation space is discretized to cells with a step size that is proportional to reconstruction accuracy (1 cm in our case). Each line-segment will vote with its length for the cell in which it is projected. So the line-segments that are perfectly parallel to road direction will vote by their total length for only one cell and the others will share their voting power between all the cells in which they are projected. The figure 5(a) depicts the initial line-segments and corresponding accumulation.

Two main signatures can be observed. The first one is a periodic high accumulation score in cells with a distance of 50 cm. The second is two high scores with about 10 cm of distance. As seen in figures 5(b) and 5(c) these two signals can be extracted by thresholding with respect to known width and length of strip. However for dashed-lines thresholding is performed with lower values. Even if all dashed-line strips vote for the same cells and cause a high score, when only few strips are available the cells score is too low. So the thresholding is performed with a lower value (the length of only one strip). As seen in the Figure 5(c) this causes some irrelevant segments to pass the filtering step. In order to cope with this problem and separate the strips of a dashed-line, a radiometric profile is computed along the dashed-line. This profile can then binarized with a threshold chosen as mean of maximum and minimum values. The outputs are sets of line-segments as candidates for each strip.

5 STRIP MODELLING

The set of line-segments for two long sides of a candidate strip is injected in the modelling step. As described in (Soheilian et al., 2006a) modelling step consists of two main tasks:

1. To model the two long sides of a parallelogram form strip if the candidates satisfy the known strip size.
2. To refine the model by searching for non-reconstructed transversal sides.

The figure 5(e) demonstrates the results of long side modelling on dashed-line strips. As regarded the extremities are not correctly reconstructed and leads to trapezoid forms. Our solution is to retrieve the transversal sides to model an optimal quasi-parallelogram. The Figure 5(f) shows the final 3D reconstructed model of the running example and the figure 6 depicts their image projection.



Figure 6: The reconstructed zebra-crossing and dashed-line.

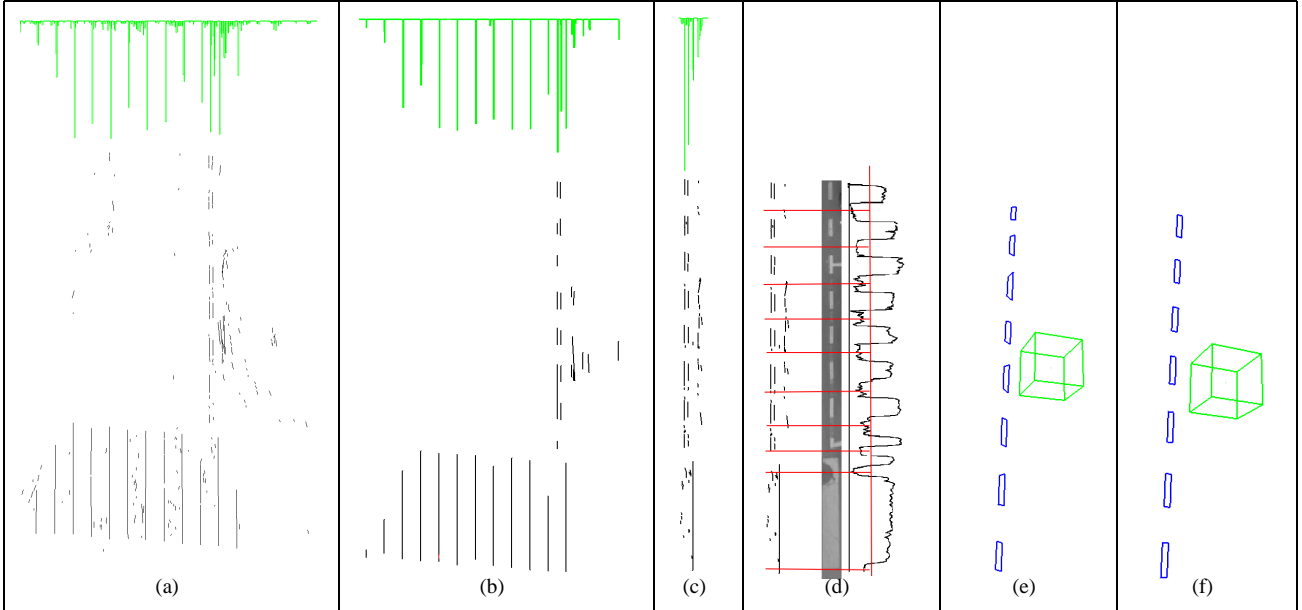


Figure 5: (a) Initial line-segments and corresponding accumulation, (b,c) zebra-crossing and dashed-line signature detection, (d) radiometric profile and strip candidates separation, (e) strips' long side modelling, (f) final strip modelling.

6 RESULTS AND EVALUATIONS

In order to evaluate the robustness and accuracy of our algorithm two kinds of evaluations are performed:

1. Geometric accuracy evaluation by computing *RMS* value for reconstructed roadmarks coordinates.
2. Completeness evaluation by computing detection, quality and false alarm rates.

6.1 Geometric accuracy evaluation

In order to test the geometric quality of the reconstructed roadmarks, some reference zebra-crossings are measured by sub-centimeter surveying methods (total stations). The reconstructed zebra-crossings are compared to the surveying measures and *RMS* is calculated on all strip corners. We reach *2 cm RMS* accuracy which is relatively higher than our *5 mm GSD* (Ground Simple Distance) at the distance of object from stereo-base. This is due to differences between the theoretical model of the object and the real object itself (non planarity, etc.)

6.2 Completeness evaluation

In order to evaluate the completeness of our algorithm, it is applied to 150 successive stereo-pairs with 4000×4000 resolution that have been acquired in the city centre of Amiens in France. The Figure 8 demonstrates some results. For each stereo-pair, the number of true-positives (TP_i), false-positives (FP_i) and strips that are visible in stereo which could be reconstructed (S_i) are counted. Three following performance measures are then computed for each type of dashed-lines and zebra-crossing.

- Detection rate: $\rho_d = \frac{\sum TP_i}{\sum S_i}$, $\rho_d \in [0, 1]$. (high values are best).
- Quality factor: $\rho_q = \frac{\sum TP_i}{\sum S_i + \sum FP_i}$, $\rho_q \in [0, 1]$. (high values are best).



Figure 7: An example of 2 false-positives for $T2$ dashed-line type.

- False alarm rate: $\rho_f = \frac{\sum FP_i}{\sum S_i}$, $\rho_f \in [0, \infty]$. (low values are best).

The results are demonstrated in Table 1. Regarding ρ_q of $T2$ dashed-line, the quality rate is very low due to large number of false-positives. It is often caused by non-roadmark objects that respect perfectly the dashed-line strips specifications. The Figure 7 present two false strips of $T2$ dashed-line type that are detected in the lighter border of road. This kind of *FP* can be filtered by a post-processing by considering stronger radiometric criteria.

7 CONCLUSION AND PERSPECTIVES

Our previous zebra-crossing reconstruction algorithm is extended to dashed-lines. The input of algorithm is a calibrated stereo-pair of images. The algorithm is fully automatic and the output is a 3D model of roadmarks. The so called algorithm is tested on a large set of images and revealed robustness, accuracy and completeness for both zebra-crossings and dashed-lines. It is quite generic and can be applied to detect and reconstruct other planar parallelograms such as windows. It can be used to generate a complete roadmark database. This database can be applied in:

1. Accurate Georeferencing of the MMS (Tournaire et al., 2006),

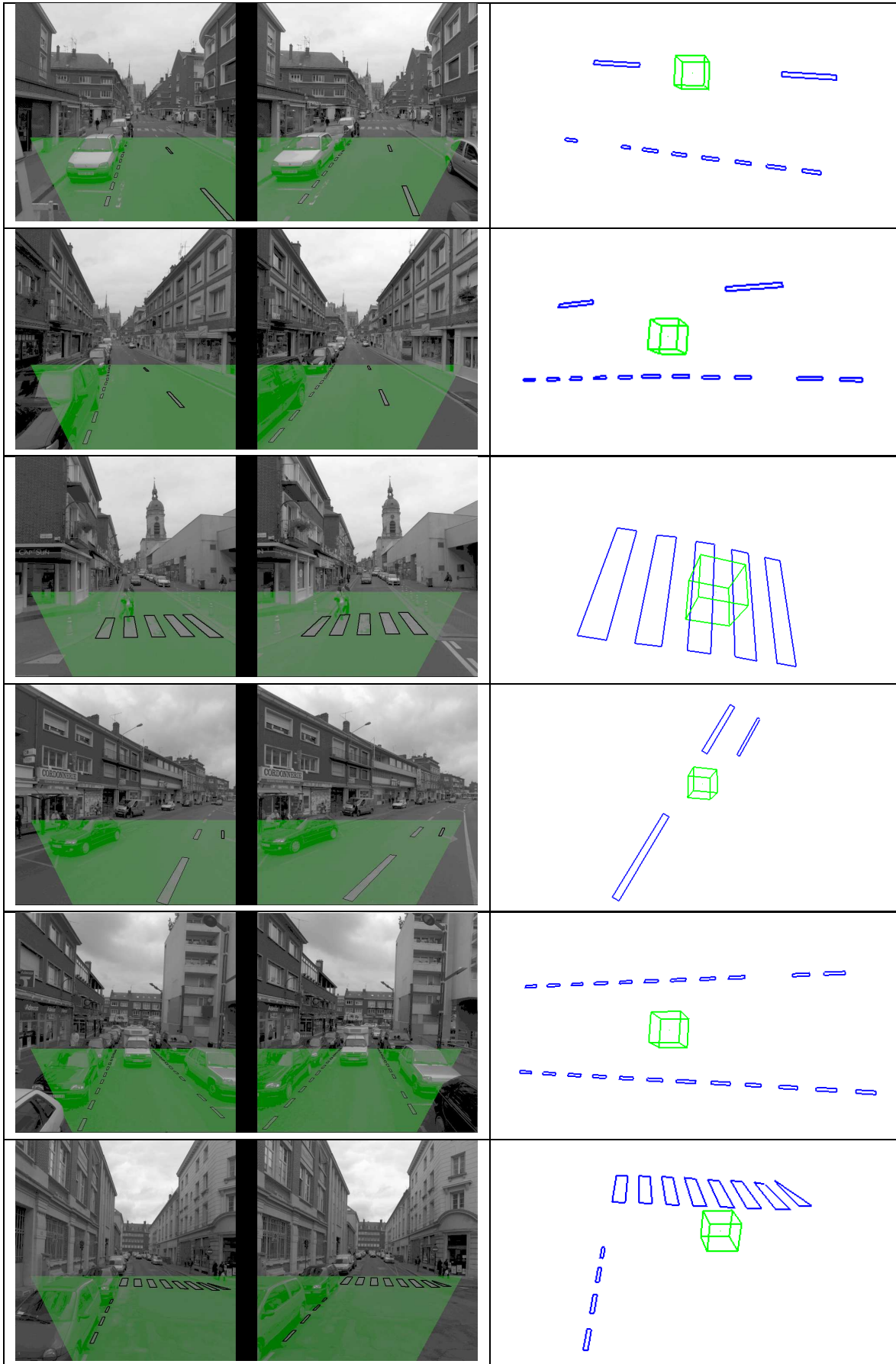


Figure 8: (Left) The stereo-image projection of reconstructed roadmarks – the overlapping region is highlighted –, (Right) 3D reconstructed roadmarks.

Type	Size (cm)	S	TP	FP	ρ_d	ρ_q	ρ_f
Dashed-lines							
T'0	10 × 50	485	416	20	86%	82%	4%
T'1	15 × 150	51	50	12	98%	79%	23%
T 3	15 × 300	30	30	2	100%	93%	7%
T 2	22 × 300	6	6	27	100%	18%	450%
Zebra-crossing							
—	50 × X	359	329	8	92%	90 %	2%

Table 1: Completeness evaluation of roadmark reconstruction.

- Roadmark GIS and autonomous navigation projects (Soheil-ian et al., 2006b).

The roadmarks are nowadays reconstructed independently in each stereo-pair. With high frame rates and thus highly overlapping images, the merging of independent results in object space will increase robustness and completeness. This is a work in progress.

REFERENCES

- Barsi, A., Lovas, T. and Kertesz, I., 2006. The potential of low-end IMUs for mobile mapping systems. In: ISPRS Commission I Symposium, From sensors to Imagery, Paris, France.
- El-Sheimy, N., 1996. A mobile multi-sensor system for gis applications in urban centers. In: The International Society for Photogrammetry and Remote Sensing (ISPRS) 1996, Commission II, Working Group, Vol. XXXI, Part B2, Vienna, Austria, pp. 95–100.
- Goulette, F., Nashashibi, F., Abuhadrous, I., Ammoun, S. and Laurgeau, C., 2006. An integrated on-board laser range sensing system for on-the-way city and road modelling. In: ISPRS Commission I Symposium, From sensors to Imagery, Paris, France.
- Paparoditis, N., Bentrach, O., Pénard, L., Tournaire, O., Soheil-ian, B. and Deveau, M., 2005. Automatic 3D recording and modeling of large scale cities: the Archipolis project. In: Modelling and Visualization of Cultural Heritage, pp. 227–235.
- Roncella, R. and Forlani, G., 2006. Automatic lane parameters extraction in mobile mapping sequences. In: Proceedings of ISPRS Commission V Symposium, image Engineering and Vision Metrology, Dresden, Germany.
- Soheil-ian, B., Paparoditis, N., Boldo, D. and Rudant, J., 2006a. 3d zebra-crossing reconstruction from stereo rig images of a ground-based mobile mapping system. In: Proceedings of ISPRS Commission V Symposium, image Engineering and Vision Metrology, Dresden, Germany. Interne.
- Soheil-ian, B., Tournaire, O., Pénard, L. and Paparoditis, N., 2006b. Different quality level processes and products for ground-based 3D city and road modeling. In: A. Abdul-Rahman, S. Zlatanov and V. Coors (eds), Lecture Notes in Geoinformation and Cartography, Innovations in 3D Geoinformation Systems, Springer-Verlag, pp. 417–429.
- Tournaire, O., Soheil-ian, B. and Paparoditis, N., 2006. Towards a sub-decimeter georeferencing of ground-based mobile mapping systems in urban areas : Matching ground-based and aerial-based imagery using roadmarks. In: ISPRS Commission I Symposium, From sensors to Imagery, Paris, France.
- Transport Ministry and Interior Ministry, 1988. Instruction inter-ministerielle sur la signalisation routiere : septième partie partie 1. Technical report.